

# Paper I

# Combining Medullary Adiposity and Cortical Porosity Identifies More Women with Nonvertebral Fractures than Either Measurement Alone

**Running head: Medullary adiposity, cortical porosity and fracture**

Marit Osima,<sup>1,2</sup> Roger Zebaze,<sup>3</sup> Minh Bui,<sup>4</sup> Marko Lukic,<sup>1</sup> Xiaofang Wang,<sup>3</sup> Ali Ghasem-Zadeh,<sup>3</sup> Erik F Eriksen,<sup>5,6</sup> Ego Seeman,<sup>3,7</sup> Åshild Bjørnerem<sup>8,9</sup>

<sup>1</sup>Department of Community Medicine, UiT The Arctic University of Norway, Tromsø, Norway

<sup>2</sup>Department of Orthopaedic Surgery, University Hospital of North Norway, Tromsø, Norway

<sup>3</sup>Departments of Medicine and Endocrinology, Austin Health, University of Melbourne, Melbourne, Australia

<sup>4</sup>Centre for Epidemiology and Biostatistics, School of Population and Global Health, University of Melbourne, Melbourne, Australia

<sup>5</sup>Department of Endocrinology, Morbid Obesity and Preventive Medicine, Oslo University Hospital, Oslo, Norway

<sup>6</sup>Department of Clinical Medicine, University of Oslo, Oslo, Norway

<sup>7</sup>Australian Catholic University, Melbourne, Australia

<sup>8</sup>Department of Clinical Medicine, UiT The Arctic University of Norway, Tromsø, Norway

<sup>9</sup>Department of Obstetrics and Gynaecology, University Hospital of North Norway, Tromsø, Norway

## Funding:

This research was facilitated through access to the Twins Research Australia, a national resource supported by an Enabling Grant (ID 628911) from the National Health & Medical Research Council (NHMRC) of Australia. This study was funded by NHMRC (Project Grant ID: 1004938) and by the Research Council of Norway (RCN) Grant (ID 178588/V50).

Corresponding author: Åshild Bjørnerem, MD, PhD

Department of Clinical Medicine, Faculty of Health Sciences

UiT The Arctic University of Norway, N-9037 Tromsø, Norway

Tel +47 4814 6064

Email:ashild.bjornerem@uit.no

## ABSTRACT

Advancing age is associated with reduction in the volume of bone formed relative to that resorbed by each remodeling unit leading to remodeling imbalance and microstructural deterioration. The reduction in bone formation may be partly due to diversion of mesenchymal cells towards adipocyte rather than osteoblast lineage cells. We therefore hypothesized that increased cortical porosity and trabecular deterioration resulting from remodelling imbalance are associated with increased medullary adiposity, and that medullary adiposity and cortical porosity are each independently associated with nonvertebral fractures, and will identify more women with fractures than either trait alone. Images were acquired at distal tibia and distal radius using high-resolution peripheral quantitative computed tomography (HR-pQCT) in 79 women aged 40-70 years with nonvertebral fractures and 345 controls in Melbourne, Australia. Medullary adiposity, cortical and trabecular morphology were quantified using StrAx software. Femoral neck (FN) areal bone mineral density (aBMD) was measured using dual-energy x-ray absorptiometry. Each standard deviation (SD) higher medullary adiposity was associated with 0.32 SD higher distal tibial cortical porosity and was nonlinearly associated with higher numbers of 0.31 SD thinner and 0.74 SD more separated trabeculae (all  $p < 0.05$ ). After adjustment for age and FN aBMD, the odds ratios (95% confidence interval) for nonvertebral fracture per SD higher medullary adiposity and cortical porosity were 3.43 (2.24-5.27) and 1.88 (1.23-2.85), respectively. Of 77 women with fractures, a medullary adiposity threshold  $>80^{\text{th}}$  percentile identified 22 women (28.6%) with fractures missed by cortical porosity, while cortical porosity threshold  $>80^{\text{th}}$  percentile identified 11 women (14.3%) missed by medullary adiposity. The sensitivity was 52.0% using distal tibia medullary adiposity, 37.7% using cortical porosity, and 66.2% using both, and specificity using both was 77.3%. Results were similar for distal radial measurements. Measuring both

medullary adiposity and cortical porosity may improve identification of women at risk for nonvertebral fractures.

**Key Words**

Cortical porosity, HR-pQCT, medullary adiposity score, nonvertebral fracture, women

## Introduction

Ageing is associated with development of abnormalities in bone remodeling (1). Around midlife in women, remodeling becomes unbalanced and rapid. Less bone is deposited than resorbed by each remodeling event resulting in microstructural deterioration. Porosity increases, cortices thin and become fragmented, trabeculae thin, perforate and may eventually disappear (2-5).

The mechanisms responsible for the reduction in the volume of bone deposited by each remodeling event are unclear. However, osteoblasts and adipocytes share common precursor cells in the bone marrow, and decreased bone formation during aging and in patients with bone fragility may be partly the result of enhanced adipogenesis compromising osteoblastogenesis (6-9). Marrow adiposity increases as age advances and is inversely associated with trabecular bone volume (10-13), but any association with cortical morphology, such as a higher cortical porosity has not been reported.

The medullary compartment of the metaphyseal region increases due to an age-related increase in unbalanced remodeling upon the endocortical surface which enlarges the medullary canal at the price of cortical thinning. The enlarged medullary canal becomes occupied by fat cells, nonfat cells and extracellular water. The proportions of this non-mineral compartment can be distinguished because fat cells attenuate photons less than the attenuation of water and non fat cells (14, 15). To quantify the proportion and density of the non-mineral compartment that is fat cells we derived a medullary adiposity score.

Cortical porosity measured at distal tibia, distal radius and the proximal femur is associated with increased fracture risk (16-18), but even when combined with areal bone mineral density (aBMD) and the Fracture Risk Assessment Tool (FRAX), more than half of the women with fractures remain unidentified (18).

As vertebral marrow adiposity is associated with compression fractures independent of aBMD, but not hip or proximal humeral fractures (12, 19), we hypothesized that: a higher medullary adiposity score is associated with higher cortical porosity and fewer trabeculae measured at the distal tibia and distal radius, and increased odds for detecting women with prevalent nonvertebral fracture. We also hypothesized that the medullary adiposity score and cortical porosity are each independently associated with nonvertebral fractures, and identifying more women with fractures than either trait alone.

## **Method**

### **Subjects**

We recruited 84 women above 40 years of age within 14 days of having had a nonvertebral fracture, to minimize the likelihood that changes in cortical porosity or medullary composition was following the fracture. These women presented to the the Emergency Department at Austin Health, Melbourne, Australia. Most fractures occurred at the distal forearm. After excluding 5 women receiving hormone replacement therapy (HRT), and 2 and 10 women with movement artifact during image acquisition of distal tibia and distal radius, 77 and 69 women with fracture remained with valid measurements of distal tibia and distal radius, respectively. We compared the measurements with those of healthy twins from the Twins Research Australia (n = 653) (3, 16, 20). Among these controls, we excluded 30 women taking HRT, 108 women below 40 years of age and 170 women with a prior fracture, 11 and 37 women with movement artifacts of distal tibia and distal radius leaving 334 and 308 controls with valid measurements of distal tibia and distal radius, respectively. The participants answered a questionnaire including information on their lifestyle, prior fracture, diseases, and use of medication. All women gave written informed consent. The Austin Health Human Research Ethics Committee approved the study.

## Measurements

Height and weight were measured while wearing light clothing and no shoes. High-resolution 3-dimensional peripheral quantitative computed tomography (HR-3D-pQCT, XtremeCT, Scanco Medical AG, Brüttisellen, Switzerland, isotropic resolution of 82  $\mu\text{m}$ ) was used to obtain images at the nondominant distal tibia and distal radius (21). In those with fracture at the nondominant side, the opposite side was scanned. The 110 CT slices were obtained at a standardized distance of 22.5 and 9.5 mm from a reference line that was manually placed at the endplate of the distal tibia and distal radius, respectively. The 49 most proximal slices in 110 slices of region of interest were chosen because the thicker cortex allows accurate assessment of cortical porosity (20).

Cortical and trabecular morphology and medullary adiposity were quantified using StrAx software (StraxCorp, Melbourne, Australia), a non-threshold based method to analyze the images that automatically segmented the bone into its compartments using curve profile analysis (22). The StrAx algorithm segments cortical bone into its compact-appearing, outer and inner transitional zones. By doing this, cortical porosity and cortical fragments that look like trabeculae produced by intracortical remodeling are both confined to the transitional zone, and not erroneously allocated to the medullary canal – a segmentation error that underestimates cortical porosity, and overestimates trabecular density (22, 23). Cortical porosity was the average void volume fraction within the compact appearing cortex, outer (OTZ) and inner transitional zones (ITZ) and total cortex (compact cortex + OTZ + ITZ) (20). Trabecular number, thickness, separation, trabecular bone volume per tissue volume (BV/TV) were quantified.

The medullary canal contains fat cells, mineralized matrix, nonfat cells and water. Voxels containing fat cells can be identified because their photons attenuation is below that of water. We expressed the fat volume (FV) as a percentage of the medullary cavity volume

(MCV) and the fat proportion (FP) =  $100 * \frac{FV}{MCV}$  (%). As age-related endocortical resorption increases the MCV, this reduces the fat proportion but not the nonmineral apparent density produced by the fat cells, nonfat cells and water. We calculated a relative medullary density (RMD) as a percentage of fully mineralized bone matrix (1200 mg HA/cm<sup>3</sup>). As the RMD becomes more negative as fat cells increase, we subtracted this value from 100 for ease of comprehension, and  $RMD (\%) = 100 - [100 * \frac{\text{Mean Medullary Density}}{1200}]$  (Fig. 1A). The Medullary Adiposity Score (MAS) is a function of the fat proportion and the relative medullary density,  $MAS = \frac{FP * RMD}{100}$ . The precision of all StrAx measurements had coefficients of variation (CV) ranged between 0.5-3.0% (22).

Femoral neck (FN) aBMD was assessed using dual-energy x-ray absorptiometry (DXA, Lunar Prodigy, Lunar Corporation, Madison, WI, USA) at the left femur, and CV was 2.6%. The women were categorized into those with normal FN aBMD (T score > -1.0), osteopenia (T-score between -2.5 and -1.0) and osteoporosis (T-score < -2.5) using the World Health Organization (WHO) classification (24).

### **Statistical analyses**

Summary statistics are presented as mean and standard deviation (SD). Cases and controls were compared using linear regression analysis for continuous data, and logistic regression analysis for binary data, adjusted for age. The associations of cortical and trabecular morphology as a function of medullary adiposity were tested in linear regression models adjusted for age, height, weight and fracture status whenever significant. Odds ratio (OR) for fracture per 1 SD change in cortical porosity, medullary adiposity and other cortical and trabecular bone morphology were calculated in logistic regression analyses adjusted for age (quadratic). In both linear and logistic regression analysis, we used the generalised estimating equations (GEE) method, which took into account the correlations within twin pairs. Distal tibia and distal radius



variables were standardised to have mean = 0 and SD = 1 in the linear and logistic regression analysis. Analyses were performed after adjustment for age and FN aBMD, and by combining cortical porosity and medullary adiposity in the same models to test whether they were independently associated with fracture. We tested the interactions between adiposity, FN aBMD and cortical porosity.

Sensitivity and specificity for fracture prevalence at the thresholds of medullary adiposity >80<sup>th</sup> percentile and cortical porosity >80<sup>th</sup> percentile were explored. Using these thresholds (with all participants as reference), we identified the proportion of women with fracture and controls meeting these criteria, and additional women identified when medullary adiposity was included. Analyses were performed using STATA Software package, v14 (StataCorp, LP, Texas, USA) and SAS software package, v9.4 (SAS Institute Inc., Cary, NC, USA). All tests were two-sided and  $p < 0.05$  considered significant.

## **Results**

### **Medullary adiposity is associated with cortical porosity and trabecular number**

Fracture cases had higher distal tibial adiposity, higher porosity of each cortical compartment, fewer and thicker trabeculae with increased separation, lower trabecular BV/TV and lower FN aBMD than controls (all  $p < 0.01$ , Table 1). Each SD higher medullary adiposity was associated with higher porosity of the compact appearing cortex by 0.14 SD, of the outer and inner transitional zones by 0.17 SD, and 0.80 SD respectively (all  $p < 0.001$ , Table 2). Medullary adiposity was associated nonlinearly with higher number of 0.31 SD thinner and 0.74 SD more separated trabeculae (all  $p < 0.05$ , Table 2). Medullary adiposity explained 0.11 to 0.66 of the variance in porosity in the compartments and 0.56 of the variance in trabecular number (Table 3). Results were similar for distal radius. All results were adjusted for age, fracture status, height and weight.

### **Medullary adiposity and cortical porosity are associated with prevalent nonvertebral fractures**

Each SD increment in medullary adiposity of distal tibia was associated with higher odds for detecting women with a prevalent nonvertebral fracture after adjustment for age (OR 3.54, 95% confidence interval (CI) 2.37-5.30, Table 4) and for FN aBMD and cortical porosity (OR 3.43, 95% CI 2.24-5.27). Each SD higher cortical porosity was associated with prevalent fracture adjusted for age (OR 2.54, 95% CI 1.82-3.57) and remained after further adjustment for medullary adiposity (OR 1.88, 95% CI 1.23-2.85). Results were similar for distal radius. There were no interactions between medullary adiposity, FN aBMD or cortical porosity.

### **Combining medullary adiposity and cortical porosity identifies additional women with prevalent fractures**

Of 77 women with prevalent fractures, 40 (52.0%) were identified using the medullary adiposity threshold of >80% percentile and 29 (37.7%) were identified using the distal tibial cortical porosity threshold of >80% percentile (Fig. 1B, Table 5). Medullary adiposity identified 22 women (28.6%) with fractures not identified by cortical porosity whereas porosity identified 11 women (14.3%) not identified by the medullary adiposity threshold; 26 (33.8%) of the women with fracture were not identified by either method.

Of 334 controls, higher medullary adiposity was present in 12.9% and higher cortical porosity was present in 16.2%. Thus, the sensitivity at these thresholds for medullary adiposity and cortical porosity was 52.0% and 37.7%, specificity was 87.1% and 83.8% (Table 5). Medullary adiposity plus cortical porosity produced a sensitivity of 66.2% and specificity 77.3%. Results were similar for distal radius. Only two of the women with fractures and five of the controls had FN osteoporosis (T-score < -2.5) (Table 1).

## Discussion

We report that women with nonvertebral fractures had higher medullary adiposity, cortical porosity and fewer, thicker and more separated trabeculae than controls. Higher medullary adiposity was associated with higher cortical porosity of each cortical compartment, particularly the inner transitional zone, and with higher numbers of thinner and more separated trabeculae. Medullary adiposity was associated with prevalent nonvertebral fractures independently of aBMD and cortical porosity. A measurement of medullary adiposity identified 28.6% additional women with fracture than identified using cortical porosity alone. For the combination of medullary adiposity and cortical porosity the sensitivity was 66.2% and specificity was 77.3%.

Most fragility fractures occur in women with osteopenia or normal aBMD, not women with osteoporosis (25). Measurement of microstructure help to identify these women and the data here and elsewhere suggest that measurement of medullary adiposity may improve the sensitivity in detecting women with osteopenia and prevalent fractures. High vertebral marrow adiposity is associated with vertebral fracture independent of aBMD (12, 19), and vertebral marrow adiposity has been reported 10% and 5% higher in patients with osteoporosis and osteopenia without fracture, respectively, compared to healthy subjects (14, 19, 26-28), suggesting a direct link between marrow adiposity and aBMD (14).

Medullary adiposity was associated with porosity of each cortical compartments, particularly of the inner transitional zone adjacent to the medullary cavity. However, the association between medullary adiposity and the porosity of the compact cortex, located more distant from the medullary cavity, is likely to be more important in compromising bending strength (29).

Medullary adiposity was also associated with higher number of thinner more separated trabeculae. However, women with fractures had fewer and more separated trabeculae with increased mean thickness, probably because thinner trabeculae were lost in women with fracture resulting in this increase in the mean value.

This study has several limitations. As it was cross-sectional, we could not assess causation between medullary adiposity, cortical and trabecular morphology and fracture. The additional women identified by medullary adiposity than by a DXA based osteoporosis threshold (T-score < -2.5 SD), could not be tested because few women with fracture as well as controls had osteoporosis.

In summary, higher medullary adiposity was associated with more porous cortices and deteriorated trabecular microstructure of distal tibia and distal radius, and a higher odds for detecting women with nonvertebral fracture independent of cortical porosity and bone mineral density of the femoral neck. Additional women with prevalent fracture were identified when medullary adiposity was combined with cortical porosity than by either measurement alone. Prospective studies are needed to determine whether adding a measurement of medullary adiposity is identifying additional women sustaining incident fracture than the assessment of bone morphology and bone mineral density alone.

## **Disclosures**

Zebaze has received grant and/or research support from Amgen, AKP, GSK, and Pfizer. He is a shareholder and a director on the board of StraxCorp. Ghasem-Zadeh is remunerated by StraxCorp as senior image analyst. Seeman has received research support and has lectured at meeting symposia funded by Amgen, Allergan, Asahi, He is a director of the board and shareholder in StraxCorp. Eriksen is a member of the advisory board for Amgen, MSD,

Novartis and Lilly and has received consulting fees from IDS, and speaker fees from Amgen, MSD, Novartis and Lilly. All authors state that they have no other conflicts of interest.

### **Acknowledgements**

This research was facilitated through access to the Australian Twin Registry, a national resource supported by an Enabling Grant (ID 628911) from the National Health & Medical Research Council (NHMRC) of Australia. This study was funded by NHMRC (Project Grant ID: 1004938) and by the Research Council of Norway (RCN) Grant (ID 178588/V50).

Authors' roles: Study design and conduct: MO, ÅB, EFE, RZ, ES. Data collection: ÅB, AGZ, XW. Responsibility for StrAx analysis: AGZ, RZ. Statistical analyses: MB, MO, ML, ÅB. Drafting manuscript: all authors. Data interpretation and approving final version of manuscript: all authors. We thank Kylie King for her excellent contribution.

## References

1. Seeman E, Delmas PD. Bone quality—the material and structural basis of bone strength and fragility. *N Engl J Med*. 2006;354(21):2250-61.
2. Seeman E. Age- and menopause-related bone loss compromise cortical and trabecular microstructure. *J Gerontol A Biol Sci Med Sci*. 2013;68(10):1218-25.
3. Bjørnerem Å, Ghasem-Zadeh A, Bui M, Wang X, Rantza C, Nguyen TV, et al. Remodeling markers are associated with larger intracortical surface area but smaller trabecular surface area: a twin study. *Bone*. 2011;49(6):1125-30.
4. Shigdel R, Osima M, Ahmed LA, Joakimsen RM, Eriksen EF, Zebaze R, et al. Bone turnover markers are associated with higher cortical porosity, thinner cortices, and larger size of the proximal femur and non-vertebral fractures. *Bone*. 2015;81:1-6.
5. Shigdel R, Osima M, Lukic M, Ahmed LA, Joakimsen RM, Eriksen EF, et al. Determinants of Transitional Zone Area and Porosity of the Proximal Femur Quantified In Vivo in Postmenopausal Women. *J Bone and Mineral Res*. 2016;31(4):758-66.
6. Moerman EJ, Teng K, Lipschitz DA, Lecka-Czernik B. Aging activates adipogenic and suppresses osteogenic programs in mesenchymal marrow stroma/stem cells: the role of PPAR- $\gamma$ 2 transcription factor and TGF- $\beta$ /BMP signaling pathways. *Aging cell*. 2004;3(6):379-89.
7. Abdallah BM, Haack-Sørensen M, Fink T, Kassem M. Inhibition of osteoblast differentiation but not adipocyte differentiation of mesenchymal stem cells by sera obtained from aged females. *Bone*. 2006;39(1):181-8.
8. Song L, Liu M, Ono N, Bringhurst FR, Kronenberg HM, Guo J. Loss of wnt/ $\beta$ -catenin signaling causes cell fate shift of preosteoblasts from osteoblasts to adipocytes. *J Bone Mineral Res*. 2012;27(11):2344-58.
9. Muruganandan S, Roman A, Sinal C. Adipocyte differentiation of bone marrow-derived mesenchymal stem cells: cross talk with the osteoblastogenic program. *Cell Mol Life Sci*. 2009;66(2):236-53.
10. Rosen CJ, Bouxsein ML. Mechanisms of disease: is osteoporosis the obesity of bone? *Nat Clin Pract Rheumatol*. 2006;2(1):35-43.
11. Justesen J, Stenderup K, Ebbesen E, Mosekilde L, Steiniche T, Kassem M. Adipocyte tissue volume in bone marrow is increased with aging and in patients with osteoporosis. *Biogerontology*. 2001;2(3):165-71.
12. Schwartz AV, Sigurdsson S, Hue TF, Lang TF, Harris TB, Rosen CJ, et al. Vertebral bone marrow fat associated with lower trabecular BMD and prevalent vertebral fracture in older adults. *J Clin Endocrinol Metab*. 2013;98(6):2294-300.
13. Devlin MJ, Rosen CJ. The bone-fat interface: basic and clinical implications of marrow adiposity. *Lancet Diabetes Endocrinol*. 2015;3(2):141-7.

14. Veldhuis-Vlug AG, Rosen CJ. Mechanisms of marrow adiposity and its implications for skeletal health. *Metabolism*. 2017;67:106-14.
15. Vogler 3rd J, Murphy W. Bone marrow imaging. *Radiology*. 1988;168(3):679-93.
16. Bjørnerem Å, Bui QM, Ghasem- Zadeh A, Hopper JL, Zebaze R, Seeman E. Fracture risk and height: an association partly accounted for by cortical porosity of relatively thinner cortices. *J Bone Miner Res*. 2013;28(9):2017-26.
17. Bala Y, Zebaze R, Ghasem- Zadeh A, Atkinson EJ, Iuliano S, Peterson JM, et al. Cortical porosity identifies women with osteopenia at increased risk for forearm fractures. *J Bone Miner Res*. 2014;29(6):1356-62.
18. Ahmed L, Shigdel R, Joakimsen R, Eldevik O, Eriksen E, Ghasem-Zadeh A, et al. Measurement of cortical porosity of the proximal femur improves identification of women with nonvertebral fragility fractures. *Osteoporos Int*. 2015:1-10.
19. Wehrli F, Hopkins J, Hwang S, Song H, Snyder P, Haddad J. Cross-sectional study of osteopenia by quantitative magnetic resonance and bone densitometry. *Radiology*. 2000;217:527-38.
20. Bjørnerem Å, Bui M, Wang X, Ghasem- Zadeh A, Hopper JL, Zebaze R, et al. Genetic and environmental variances of bone microarchitecture and bone remodeling markers: a twin study. *J Bone Miner Res*. 2015;30(3):519-27.
21. Laib A, Häuselmann HJ, Rüeggsegger P. In vivo high resolution 3D-QCT of the human forearm. *Technol Health Care*. 1998;6(5-6):329-37.
22. Zebaze R, Ghasem-Zadeh A, Mbala A, Seeman E. A new method of segmentation of compact-appearing, transitional and trabecular compartments and quantification of cortical porosity from high resolution peripheral quantitative computed tomographic images. *Bone*. 2013;54(1):8-20.
23. Zebaze RM, Ghasem-Zadeh A, Bohte A, Iuliano-Burns S, Mirams M, Price RI, et al. Intracortical remodelling and porosity in the distal radius and post-mortem femurs of women: a cross-sectional study. *Lancet*. 2010;375(9727):1729-36.
24. Looker AC, Orwoll ES, Johnston CC, Lindsay RL, Wahner HW, Dunn WL, et al. Prevalence of low femoral bone density in older US adults from NHANES III. *J Bone Miner Res*. 1997;12(11):1761-8.
25. Siris ES, Chen Y-T, Abbott TA, Barrett-Connor E, Miller PD, Wehren LE, et al. Bone mineral density thresholds for pharmacological intervention to prevent fractures. *Arch Intern Med*. 2004;164(10):1108-12.
26. Yeung DKW, Griffith JF, Antonio GE, Lee FKH, Woo J, Leung PC. Osteoporosis is associated with increased marrow fat content and decreased marrow fat unsaturation: A proton MR spectroscopy study. *J Magn Reson Imaging*. 2005;22(2):279-85.

27. Griffith JF, Yeung DK, Antonio GE, Wong SY, Kwok TC, Woo J, et al. Vertebral marrow fat content and diffusion and perfusion indexes in women with varying bone density: MR evaluation. *Radiology*. 2006;241(3):831-8.
28. Li X, Kuo D, Schafer AL, Porzig A, Link TM, Black D, et al. Quantification of vertebral bone marrow fat content using 3 Tesla MR spectroscopy: reproducibility, vertebral variation, and applications in osteoporosis. *J Magn Reson Imaging*. 2011;33(4):974-9.
29. Seeman E. Growth and age-related abnormalities in cortical structure and fracture risk. *Endocrinol Metab (Seoul)*. 2015;30(4):419-28.



**Table 1.** Characteristics of women by fracture status

	<b>Cases</b>	<b>Controls</b>	
	n = 79	n = 345	p
Age (years)	54.5 ± 6.5	50.6 ± 8.5	< 0.001
Height (cm)	162.6 ± 6.4	162.7 ± 6.3	0.775
Weight (kg)	72.2 ± 14.7	70.3 ± 15.6	0.334
Femoral neck (FN) aBMD (mg/cm <sup>2</sup> )	0.89 ± 0.13	0.97 ± 0.15	< 0.001
FN normal aBMD, n (%)	45 (57.7)	264 (77.4)	0.003
FN osteopenia, n (%)	31 (39.7)	72 (21.1)	0.004
FN osteoporosis, n (%)	2 (2.56)	5 (1.47)	0.470
<b>Distal Tibia</b>	n = 77	n = 334	
Total cortical porosity (%)	64.5 ± 5.8	59.7 ± 6.1	< 0.001
Compact cortex porosity (%)	46.7 ± 7.4	41.8 ± 7.1	< 0.001
Outer transitional zone porosity (%)	47.5 ± 6.6	42.8 ± 6.2	< 0.001
Inner transitional zone porosity (%)	87.1 ± 3.2	84.6 ± 3.1	< 0.001
Cortical thickness (mm)	2.36 ± 0.31	2.34 ± 0.24	0.410
Trabecular number (1/mm)	2.15 ± 0.51	2.77 ± 0.65	< 0.001
Trabecular thickness (mm)	0.20 ± 0.01	0.19 ± 0.01	0.001
Trabecular separation (mm)	1.58 ± 0.31	1.32 ± 0.29	< 0.001
Trabecular bone volume/tissue volume (%)	2.93 ± 1.46	4.14 ± 1.71	< 0.001
Medullary adiposity score	43.5 ± 3.2	39.9 ± 3.9	< 0.001
<b>Distal Radius</b>	n = 69	n = 308	
Total cortical porosity (%)	57.8 ± 5.3	53.5 ± 6.2	< 0.001
Compact cortex porosity (%)	40.4 ± 5.3	36.3 ± 5.6	< 0.001
Outer transitional zone porosity (%)	43.6 ± 4.9	39.9 ± 4.9	< 0.001
Inner transitional zone porosity (%)	86.9 ± 2.7	84.5 ± 2.9	< 0.001
Cortical thickness (mm)	1.82 ± 0.19	1.81 ± 0.20	0.526
Trabecular number (1/mm)	1.88 ± 0.55	2.35 ± 0.50	< 0.001
Trabecular thickness (mm)	0.20 ± 0.01	0.19 ± 0.01	0.017
Trabecular separation (mm)	1.65 ± 0.36	1.36 ± 0.30	< 0.001
Trabecular bone volume/tissue volume (%)	1.84 ± 1.14	3.03 ± 1.57	< 0.001
Medullary adiposity score	48.4 ± 3.3	44.1 ± 4.2	< 0.001

Numbers are mean ± standard deviation, or number (%).

Cases and controls were compared using generalised estimating equations (GEE) and adjusted for age. aBMD = areal bone mineral density.

**Table 2.** Association of a 1 SD increment in medullary adiposity score (predictors) with cortical and trabecular traits of distal tibia and distal radius (outcomes)

Outcome variables	Distal tibia			Distal radius		
	Coefficient	SE	p	Coefficient	SE	p
Total cortical porosity (%)	0.32	0.04	< 0.001	0.36	0.05	< 0.001
Compact cortex porosity (%)	0.14	0.04	< 0.001	0.20	0.05	< 0.001
Outer transitional zone porosity (%)	0.17	0.04	< 0.001	0.23	0.04	< 0.001
Inner transitional zone porosity (%)	0.80	0.03	< 0.001	0.79	0.03	< 0.001
Cortical thickness (mm)	-0.09	0.05	0.076	-0.11	0.05	0.024
Trabecular number (1/mm) - linear	-1.41	0.40	< 0.001	-0.71	0.03	< 0.001
- quadratic	0.83	0.40	0.041			
Trabecular thickness (mm)	-0.31	0.05	< 0.001	-0.30	0.05	< 0.001
Trabecular separation (mm) - linear	0.74	0.03	< 0.001	0.81	0.03	< 0.001
Trabecular BV/TV (%) - linear	-2.73	0.26	< 0.001	-3.34	0.35	< 0.001
- quadratic	1.78	0.26	< 0.001	2.44	0.35	< 0.001

Linear regression models using generalised estimating equations (GEE) to fit data, adjusted for age, height, weight and fracture status whenever significant. All variable were standardized to have mean = 0 and standard deviation (SD) = 1. SE = standard error of the mean.

**Table 3.** Association of a 1 SD increment in medullary adiposity score (predictors) with cortical and trabecular traits of distal tibia and distal radius (outcomes), presented unadjusted for confounders, and with the variance in cortical and trabecular traits that is explained by the medullary adiposity

Outcome variables	Distal tibia			Distal radius		
	Coefficient	p	R <sup>2</sup>	Coefficient	p	R <sup>2</sup>
Total cortical porosity (%)	0.46	< 0.001	0.23	0.44	<0.001	0.22
Compact cortex porosity (%)	0.27	< 0.001	0.11	0.30	<0.001	0.14
Outer transitional zone porosity (%)	0.28	< 0.001	0.15	0.33	<0.001	0.17
Inner transitional zone porosity (%)	0.82	< 0.001	0.66	0.81	<0.001	0.67
Cortical thickness (mm)	-0.11	0.024	0.01	-0.12	0.017	0.02
Trabecular number (1/mm) - linear	-0.73	<0.001	0.56	-0.74	<0.001	0.56
Trabecular thickness (mm)	-0.13	0.005	3.3x10 <sup>-7</sup>	-0.14	0.003	0.01
Trabecular separation (mm) - linear	0.79	<0.001	0.64	0.83	<0.001	0.67
Trabecular BV/TV (%) - linear	-2.86	<0.001	0.86	-3.44	<0.001	0.89
- quadratic	1.94	<0.001		2.56	<0.001	

Linear regression models using generalised estimating equations (GEE) to fit data. All variables were standardized to have mean = 0 and standard deviation (SD) = 1. Explained variance, R<sup>2</sup> = r-square.

**Table 4.** Fracture risk by 1 standard deviation (SD) increment in cortical and trabecular bone morphology of distal tibia and distal radius

	Odds Ratio (95% CI)	p
<b>Univariate analysis</b>		
Age (years) - linear	3.12 (1.88-5.16)	< 0.001
- quadratic	0.99 (0.986-0.995)	< 0.001
Height (cm)	1.00 (0.96-1.04)	0.835
Weight (kg)	1.01 (0.99-1.02)	0.310
Femoral neck (FN) aBMD (mg/cm <sup>2</sup> )	0.53 (0.40-0.69)	< 0.001
<b>Age-adjusted analysis</b>		
<b>Distal tibia</b>		
Total cortical porosity (%)	2.54 (1.82-3.57)	< 0.001
Compact cortex porosity (%)	2.09 (1.53-2.87)	< 0.001
Outer transitional zone porosity (%)	2.41 (1.69-3.43)	< 0.001
Inner transitional zone porosity (%)	2.12 (1.51-2.97)	< 0.001
Cortical thickness (mm)	1.17 (0.90-1.53)	0.249
Trabecular number (1/mm)	0.32 (0.23-0.46)	< 0.001
Trabecular thickness (mm)	1.77 (1.35-2.33)	0.002
Trabecular separation (mm)	2.18 (1.63-2.91)	< 0.001
Trabecular bone volume/tissue volume (%)	0.41 (0.27-0.62)	< 0.001
Medullary adiposity score	3.54 (2.37-5.30)	< 0.001
<b>Distal radius</b>		
Total cortical porosity (%)	2.30 (1.67-3.17)	< 0.001
Compact cortex porosity (%)	2.36 (1.65-3.38)	< 0.001
Outer transitional zone porosity (%)	2.74 (1.84-4.09)	< 0.001
Inner transitional zone porosity (%)	2.31 (1.63-3.28)	< 0.001
Cortical thickness (mm)	1.02 (0.79-1.31)	0.882
Trabecular number (1/mm)	0.39 (0.27-0.56)	< 0.001
Trabecular thickness (mm)	1.74 (1.29-2.34)	< 0.001
Trabecular separation (mm)	2.16 (1.61-2.90)	< 0.001
Trabecular bone volume/tissue volume (%)	0.35 (0.22-0.55)	< 0.001
Medullary adiposity score	4.18 (2.66-6.57)	< 0.001

Logistic regression models using generalised estimating equations (GEE) to fit the data, and the models of distal tibia and distal radius variables were adjusted for age (quadratic). Distal tibia and distal radius variables were standardised to have mean = 0 and SD = 1.

**Table 5.** Sensitivity and specificity with 95% confidence interval (CI) for fracture at selected thresholds for medullary adiposity score and cortical porosity and for the combination of medullary adiposity score and cortical porosity

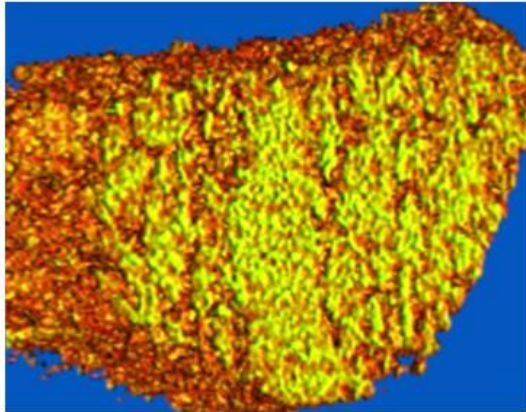
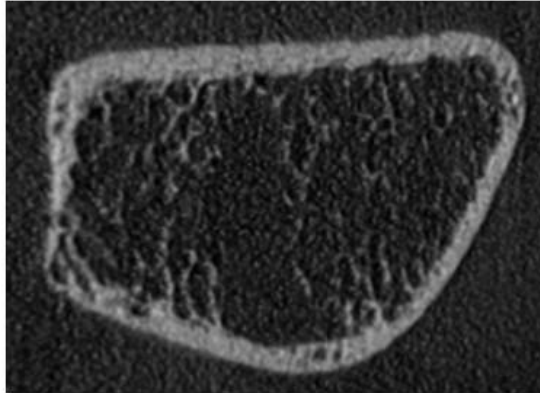
	Sensitivity (%)	95% CI	Specificity (%)	95% CI
<b>Distal tibia</b>				
Medullary adiposity >80 <sup>th</sup> percentile	52.0	41.8-62.0	87.1	78.6-92.7
Cortical Porosity >80 <sup>th</sup> percentile	37.7	28.4-48.0	83.8	74.8-90.1
Cortical porosity or medullary adiposity >80 <sup>th</sup> percentile*	66.2	56.0-75.2	77.3	67.6-84.8
<b>Distal radius</b>				
Medullary adiposity >80 <sup>th</sup> percentile	50.7	40.6-60.8	86.7	78.1-92.4
Cortical Porosity >80 <sup>th</sup> percentile	36.2	27.0-46.5	83.4	74.3-89.8
Cortical porosity or medullary adiposity >80 <sup>th</sup> percentile*	65.2	54.9-74.3	75.7	65.9-83.5

\*When cortical porosity was combined with medullary adiposity and one or the other trait was >80<sup>th</sup> percentile.

**Fig. 1A.** Fat voxels in the medullary cavity are color-coded in a scale ranging from red to yellow depending on their attenuation relative to water. The larger the proportion of yellow bone marrow (fat cells) than red bone marrow (hematopoietic cells), the lower is the density.

**Fig. 1B.** Venn diagrams illustrate number and proportion of women identified using threshold for medullary adiposity score  $>80^{\text{th}}$  percentiles and cortical porosity  $>80^{\text{th}}$  percentiles in 77 fracture cases and 334 controls with valid distal tibia measurements.

**A** 3D display of the medullary cavity at distal radius



Yellow bone marrow

Red bone marrow

